Journal of Power Sources 252 (2014) 317–326

Contents lists available at ScienceDirect

Journal of Power Sources

journal homepage: www.elsevier.com/locate/jpowsour

Gas phase recovery of hydrogen sulfide contaminated polymer electrolyte membrane fuel cells

Biraj Kumar Kakati, Anthony R.J. Kucernak*

Department of Chemistry, Imperial College London, London SW7 2AZ, UK

HIGHLIGHTS

- Recovery of H_2S contaminated PEMFC is studied via external polarization and O_3 cleaning.
- The room temperature O_3 cleaning process completely rejuvenates the H_2S contaminated fuel cell in 600–900 s.
- O_3 cleaning at room temperature avoids excessive carbon corrosion as seen by low CO_2 generation.
- The in-situ O_3 cleaning process proceeds through both a chemical and electrochemical route.

GRAPHICAL ABSTRACT

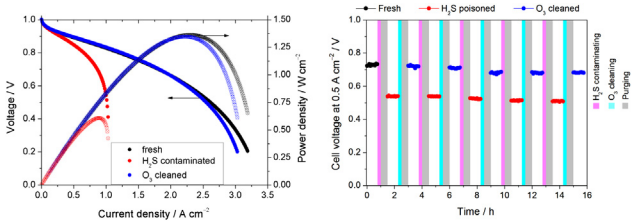

ARTICLE INFO

Article history:
Received 28 July 2013
Received in revised form
4 November 2013
Accepted 22 November 2013
Available online 11 December 2013

Keywords:
Cyclic voltammetry
Electrochemical surface area
Gas phase recovery
H_2S contamination
Ozone
Polymer electrolyte membrane fuel cell

ABSTRACT

The effect of hydrogen sulfide (H_2S) on the anode of a polymer electrolyte membrane fuel cell (PEMFC) and the gas phase recovery of the contaminated PEMFC using ozone (O_3) were studied. Experiments were performed on fuel cell electrodes both in an aqueous electrolyte and within an operating fuel cell. The ex-situ analyses of a fresh electrode; a H_2S contaminated electrode (23 μmol_{H_2S} cm^{-2}); and the contaminated electrode cleaned with O_3 shows that all sulfide can be removed within 900 s at room temperature. Online gas analysis of the recovery process confirms the recovery time required as around 720 s. Similarly, performance studies of an H_2S contaminated PEMFC shows that complete rejuvenation occurs following 600–900 s O_3 treatment at room temperature. The cleaning process involves both electrochemical oxidation (facilitated by the high equilibrium potential of the O_3 reduction process) and direct chemical oxidation of the contaminant. The O_3 cleaning process is more efficient than the external polarization of the single cell at 1.6 V. Application of O_3 at room temperature limits the amount of carbon corrosion.

Room temperature O_3 treatment of poisoned fuel cell stacks may offer an efficient and quick remediation method to recover otherwise inoperable systems.

1. Introduction

The polymer electrolyte membrane fuel cell (PEMFC) is considered to be the one of the most promising portable power sources due to its fast start-up, high power density, quick load following, and ease of electrolyte handling, low corrosion and system robustness [1–4]. The purity of the hydrogen (H_2) should be relatively high to achieve high efficiency, power density and long

* Corresponding author. Tel.: +44 20 75945831; fax: +44 20 75945804.
E-mail address: anthony@imperial.ac.uk (A.R.J. Kucernak).

0378-7753
http://dx.doi.org/10.1016/j.jpowsour.2013.11.077

life time. Nowadays, H_2 is produced most likely from fossil fuels, through steam reforming of methane and partial oxidation of hydrocarbon fuels. The reformed hydrogen might have various impurities like nitrogen, CO_x, NO_x, SO_x, ammonia, hydrogen sulfide (H_2S) and trace amount of hydrocarbons [5]. The PEMFC research involving fuel side contaminants are mainly focused on the effects of CO and tolerance to it [6–20]. In the case of sulfides, more precisely H_2S, research is mainly focused on the effects of the contaminant on the electrochemical performance of the catalyst or on the performance of the fuel cell [21–26]. Unlike CO, the detrimental effect of H_2S on the performance of the fuel cell is cumulative and highly irreversible [23,27]. Furthermore, the normal CO mitigation approaches, better known as Pt–Ru alloy catalyst and/or air bleeding, do not provide a satisfactory remedy for H_2S contamination [21]. The first experimental work on the contamination of platinum catalyst by sulfur compound was carried out by Loučka et al., in 1971 [28,29]. Heinzel et al. (2002) reported a decrease in cell performance due to the presence of H_2S at as low a concentration as 0.5 ppm [30].

The in-situ research on the effect of sulfides on the performance of PEMFC has been performed [21,31–37]. However, only a handful of literature studies are available on the effort to recover H_2S contaminated fuel cells [32,38–40]. Uribe et al. (2001) reported that a partial recovery could be achieved by potential scanning of the electrode between 0 and 1.4 V vs dynamic hydrogen electrode [27]. Mohtadi et al. [21] reported that the degree of recovery of a PEMFC anode contaminated with H_2S depended on the degree of oxidation of the two surface species Pt–S and Pt–S_2. They later studied the effect of operating temperature on the severity of the contamination of fuel cell with H_2S [41]. The presence of two forms of chemisorbed sulfur on platinum was reported by Contractor and Lal [42]. Shi et al. [40] carried forward the study on the severity of H_2S poisoning on the performance of fuel cell with different H_2S concentration, current density and the cell temperature. They used a high voltage pulse to recover the performance of the 5 ppm H_2S contaminated fuel cell [39]. Gould et al. used potential cycling and potential hold techniques to study the recovery of SO_2 [32] and H_2S [25] contaminated PEMFCs in nitrogen and air environments. They reported that partial recovery of PEMFC polarization curve performance (92% of original power at 0.6 V) was possible but strongly dependent on the external polarization program. It seems clear that electrokinetic remediation or external polarization (cycling and/or potential hold) of the contaminated cell is not a viable solution for a large stack.

In this paper we report the use of a gaseous reactant, ozone (O_3), as a means to treat a fuel cell poisoned with H_2S. This process does not require external polarization of the cell and thus can easily be performed on a fuel cell stack. Although we use H_2S as an example of a poison, this process might equally be applicable to other poisons. For instance, it is interesting to note that SO_2 seems to follow a similar pathway in deposition of S_{ads} on platinum, so the remediation process we describe here would also be suitable for fuel cell electrodes exposed to SO_2 [42].

2. Experimental

2.1. Materials

ACS reagent grade sulfuric acid (95%), hydrogen peroxide (35 wt.%), potassium permanganate (99%), and anhydrous propan-2-ol (99.5%) were procured from Sigma–Aldrich, UK. Ultra-pure water (Millipore Milli-Q, 18.2 MΩ cm) was used to prepare various solutions. Fuel cell electrodes with a nominal Pt loading of 0.4 mg cm^{-2} were from Alfa Aesar, UK. Nafion PFSA NR212 membranes were procured from DuPont, USA. Hydrogen, Oxygen, Nitrogen, and 1000 ppm H_2S in Argon cylinders were procured from Air Products. Compressed air was used for fuel cell testing. The N6 grade gas cylinders were controlled with N6 rated regulators (GCE Druva and Air products) and connected with specially cleaned (SC-11) tubing and fittings from Swagelok. Room temperature during experimental measurements was 25 ± 2 °C.

2.2. Electrochemical measurements

Experiments in this paper have been performed in both a three-electrode electrochemical cell utilizing an aqueous acid electrolyte (ex-situ measurements), and within a fuel cell (in situ measurements). The electrodes used in the three-electrode electrochemical cell were the same as those used in the fuel cell and were poisoned and cleaned with O_3 in an external flow-field (Fig. 1(b)) in order to (a) replicate the process that occurs within a fuel cell; and (b) avoid contamination of the electrochemical cell by hydrogen sulfide or O_3 during the experiments. The only time that O_3 was utilized in the three-electrode electrochemical cell was during the measurements of the open circuit potential (OCV) of the electrode during exposure to O_3 (Fig. 3(a)).

2.2.1. Ex-situ electrochemical analysis of fuel cell electrodes

The glassware was rigorously cleaned before using for any electrochemical analysis. The glassware was initially soaked in acidified $KMnO_4$ for 12 h, followed by rinsing with acidified H_2O_2 and ultra-pure water, respectively. The glassware was again soaked in piranha solution for 6 h and thoroughly washed with ultra-pure water before use. All the ex-situ electrochemical analyses were carried out in 1.0 M H_2SO_4 solution in a 5 neck jacketed cell. All electrochemical measurements were carried out using a Potentiostat/Galvanostat/ZRA (Reference 3000, Gamry, USA). For aqueous electrochemical studies, the working electrode was a 1 cm^2 of fuel cell electrode (Johnson Matthey, Alfa Aesar catalog # 45372, 0.4 mg_{Pt} cm^{-2}) in a platinum wire holder. A high surface area Pt-wire was used as a counter electrode and a reversible hydrogen electrode was used as a reference electrode (HydroFlex®; Gaskatel GmbH, Germany). Fig. 1(a) shows the schematic of the ex-situ electrochemical cell of the fuel cell electrodes. All the ex-situ cyclic voltammetry (CV) analyses were carried out at room temperature (25 ± 2 °C), unless otherwise specified. The electrochemical surface areas (ECA) of the electrode were calculated from the hydrogen desorption area in the cyclic voltammetry [43]. Further discussion is provided in supplementary material.

2.2.2. H_2S contamination and O_3 recovery in an ex-situ flowfield

For all the ex-situ electrochemical experiments, the H_2S contamination and O_3 cleaning processes were carried out at room temperature utilizing an external flowfield, Fig. 1(b). The electrode was placed in a flowfield (parallel channels, 1 mm land, 1 mm channel) and the relevant gases were passed over its surface. Flow rates of 75 sccm were used, which in this geometry corresponds to a space velocity of 12.5 s^{-1}. Utilizing an external flowfield for the contamination and cleaning processes avoided contamination of the electrolyte, RHE, and counter electrodes with H_2S. The external flowfield was purged with N_2 after contaminating the electrode with H_2S (100 ppm, balance hydrogen, effective dose 23 μmol cm^{-2}) and again after O_3 treatment. After contamination and/or cleaning with O_3, the electrode was transferred from the flowfield to the electrochemical cell for characterization. The effective dose is calculated assuming all the H_2S is absorbed by the electrode and none leaves the flowfield.

The O_3 cleaning process of the H_2S contaminated electrode was monitored with the help of an online gas analyzer (HPR-20 QIC Hiden analytical, UK). The mass spectrometer was typically allowed

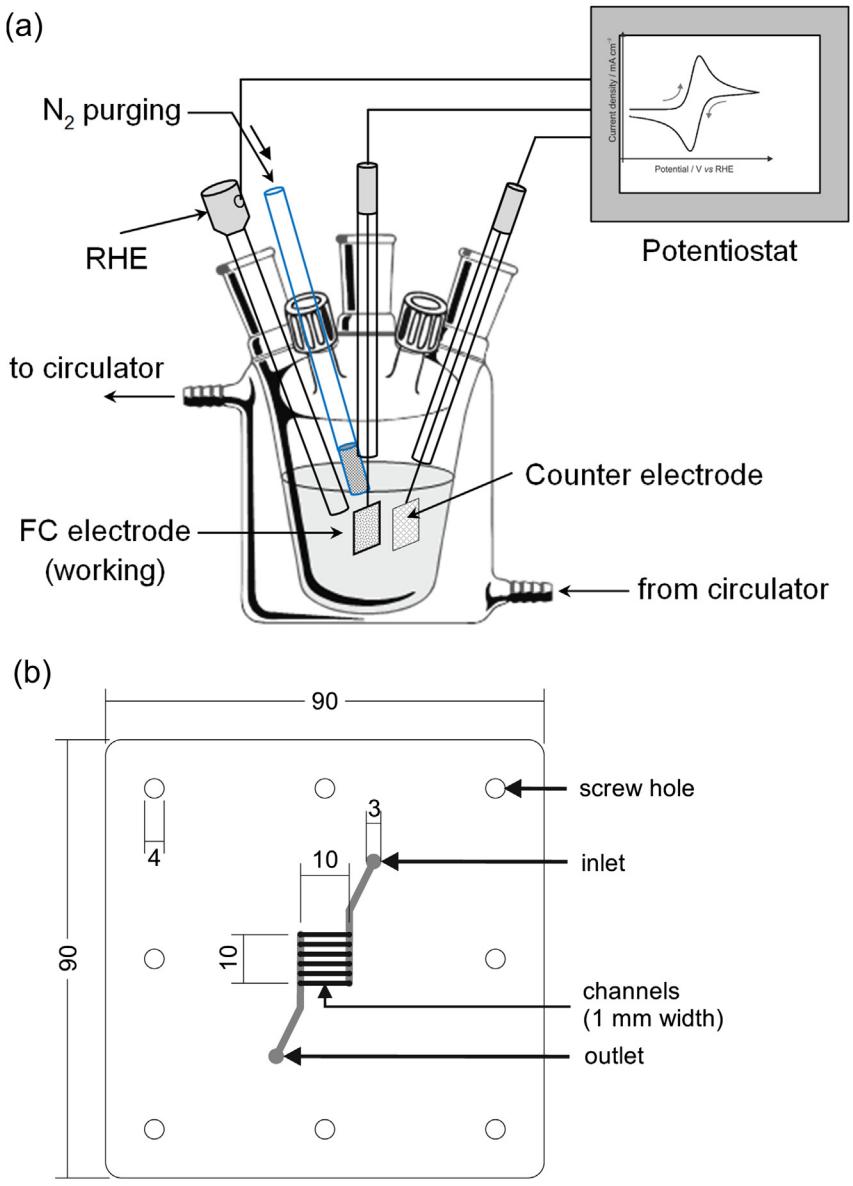

Fig. 1. (a) Schematic of ex-situ electrochemical analysis of fuel cell electrodes; (b) schematic of flowfields used in poisoning and ex-situ O_3 regeneration studies (all the dimensions are in mm). The gray channels are inside the flow-field plate.

to stabilize for two hours to reach a steady state before measurements were taken. The O_3 required for the experiments were produced using an O_3 generator (model: BMT801; make: BMT Messtechnik GmbH, Germany). The O_3 concentration produced by the generator was measured using an UV/Vis dual beam spectrometer (UV4-200, ATI-Unicam) at the known ozone UV absorption peak ($\lambda_{max} = 253.7$; $\varepsilon = 3000 \pm 30$ dm^3 mol^{-1} cm^{-1}) [44].

2.3. In-situ H_2S contamination, O_3 recovery, and fuel cell operation

A standard procedure was followed for pretreatment of the Nafion membranes [45]. The pretreated membrane was sandwiched between two electrodes (2.1 × 2.1 cm^2 in size, Johnson Matthey, Alfa Aesar catalog # 45372, 0.4 mg$_{Pt}$ cm^{-2}) and hotpressed at 160 °C under 5 MPa pressure for 210 s. The prepared MEA was

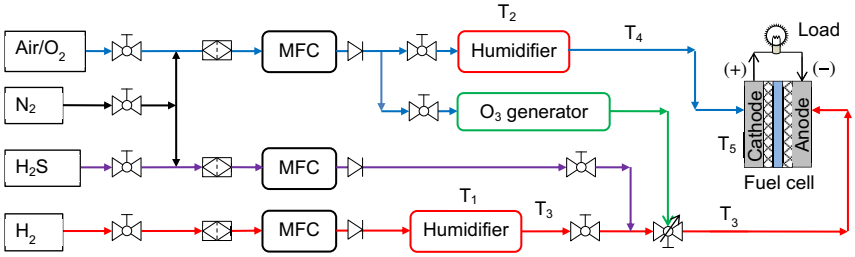

Fig. 2. Schematic of fuel cell setup used to study the H_2S contamination and O_3 recovery process; T_i-s are temperature controller used at different parts of the fuel cell setup.

then used in fuel cell hardware (FC-01-02; Electrochem Inc., USA) for further studies. A schematic of the fuel cell setup used for the contamination-recovery studies is shown in Fig. 2. The fuel cell was operated at 70 °C for performance measurements and poisoning. During rejuvenation of the electrode with O_3 the fuel cell was operated at room temperature. The H_2 and O_2 or air stoichiometries were maintained at 1.5 and 2.5 relative to the maximum current densities, respectively. The developed cells were galvanostatically broken-in for 8–12 h at 1.0 A cm^{-2} current density with neat H_2 and O_2 as anode and cathode gases. During measurement of performance curves, the current density was increased with the output voltage of the cell recorded 900 s after reaching each specified current density. The contamination studies were carried out by diluting 1000 ppm H_2S in Argon with hydrogen downstream of the humidifier. The dose of H_2S to the fuel cell electrode is calculated at 23 μmol cm^{-2} assuming all the H_2S is adsorbed.

The offline O_3 recovery process was carried out by switching off the hydrogen stream, purging the anode with nitrogen followed by passing an oxygen stream through the O_3 generator (as described above). The recovery process was performed at room temperature, A fuel cell load/impedance analyzer (KFM2030; Kikusui, Japan) was used for polarization and performance studies of the fuel cell. For in-situ electrochemical measurements, the cathode of the fuel cell was purged with hydrogen and connected to the Gamry potentiostat as counter/reference, and the anode was purged with Nitrogen and connected as working electrode.

2.4. Contact angle measurement

The contact angles on the fresh, H_2S contaminated, and O_3 treated electrodes were analyzed using a drop shape analyzer (DSA10; Kruss GmbH, Germany).

3. Results and discussion

3.1. Ex-situ cyclic voltammetry of the fuel cell electrode

Cyclic voltammetry was used to monitor the quality of the platinum catalyst for the fresh, H_2S contaminated, and O_3-cleaned electrodes. It has already been reported in several papers that external polarization can partially remove the adsorbed S from the Pt catalyst [28,38,40,41,46].

The CVs of a fresh, an H_2S contaminated, and a contaminated and then O_3-cleaned electrodes are shown in Fig. 3(b). The CVs of the electrochemically cleaned electrodes are shown with a dashed curve. The anodic peak at 163 mV (labeled 1) is attributed to the weakly bonded hydrogen atom at Pt(110). The other anodic peak at 273 mV (labeled 2) is usually attributed due to the strongly bonded hydrogen atom on the Pt(100) crystal facets. The peak due to the hydrogen adsorption at Pt(111) happens to merge with the above two peaks with preferential contribution to the first peak [47]. The slightly bulged region between the two anodic peaks (labeled 3) is attributed to the sub-surface molecular hydrogen [48]. The flat peak in between 0.5 and 0.6 V (labeled 4) is attributed to the hydroquinone-quinone redox couple due to surface oxidation of carbon supports [49]. The average ECA of the fresh electrode was calculated to be 89.0 m^2 g^{-1} of Pt, based on the manufacturers platinum loading. The electrode was then transferred to the external flow-field and subjected to 100 ppm H_2S/H_2 for 900 s at room temperature (a dose of 23 μmol cm^{-2}). The innermost curve in Fig. 3(a) represents the CV of the H_2S contaminated electrode. It is observed that the hydrogen adsorption and desorption peaks are totally suppressed on the H_2S poisoned electrode. The reaction of H_2S with the Pt catalyst can be realized by the following reactions.

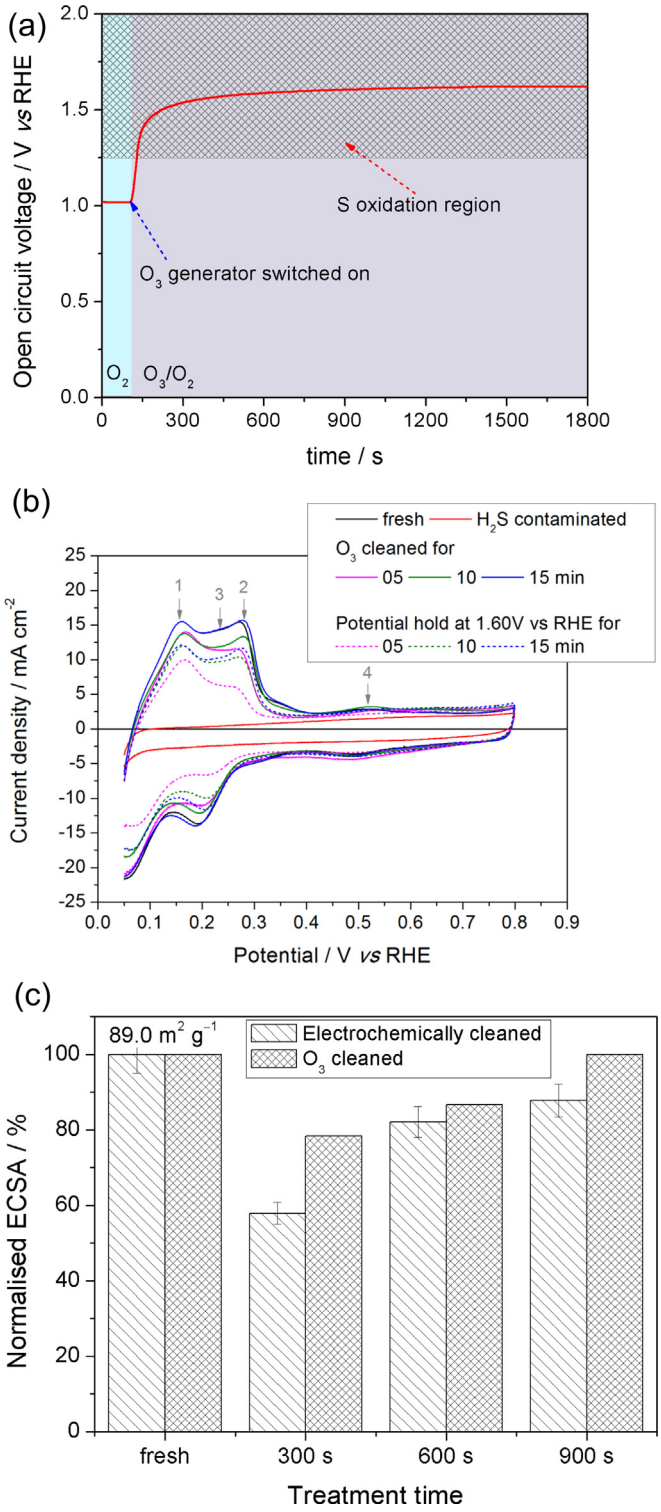

Fig. 3. (a) Variation of open circuit potential for a clean electrode in 1.0 mol dm^{-3} H_2SO_4 in the electrochemical cell when the gas bubbling through the electrolyte is changed from pure oxygen to 2 vol% O_3 in O_2; (b) Cyclic voltammograms of fresh, H_2S poisoned (in external flowfield, 100 ppm H_2S, balance hydrogen, 900 s, effective dose 23 μmol cm^{-2}), O_3 cleaned (in external flowfield, 2 vol% O_3 in O_2), and potential hold (1.6 V in aqueous electrolyte electrochemical cell) cleaned fuel cell electrodes. Each voltammogram was performed on a fresh electrode; (c) normalized ECSA for the fresh and cleaned electrodes. Error bars correspond to standard deviation for ten replicates of the experiment. Voltammetry performed in 1.0 mol dm^{-3} H_2SO_4 with a 40 mV s^{-1} scan rate. All experiments performed at room temperature.

$$Pt + H_2S \rightleftharpoons Pt - H_2S_{ads} \quad (1)$$

$$Pt - H_2S_{ads} \rightleftharpoons Pt - S + H_2 \quad (2)$$

In a dry environment, reactions (1) and (2) are likely to occur, as confirmed by experiments on H_2S reaction on 2 nm diameter Pt on Al_2O_3 at room temperature in the absence of H_2 in the initial reactant gas [50]. However in presence of water, the sulfur may also be deposited on the Pt catalyst following reactions (3)–(5) [51].

$$H_2S + H_2O \rightleftharpoons S^- + H_3O^+ \quad \log\left(\frac{HS^-}{H_2S}\right) = -7 + pH \quad (3)$$

$$HS^- + H_2O \rightleftharpoons S^{2-} + H_3O^+ \quad \log\left(\frac{S^{2-}}{HS^-}\right) = -13.9 + pH \quad (4)$$

$$S + 2H^+ + 2e^- \rightleftharpoons H_2S_{(aq)} \quad E^o = 0.142\ V \quad (5)$$

$$S + H^+ + 2e^- \rightleftharpoons HS^-_{(aq)} \quad E^o = -0.065\ V \quad (6)$$

$$Pt - S_{ads} + 2H^+ + 2e^- \rightleftharpoons Pt + H_2S_{(aq)} \quad E^o = \text{unknown} \quad (7)$$

H_2S is a poor acid, eq (3), and so the concentration of HS^- will be vanishingly small in the ionomer over the catalyst where the pH ~ 0. However, within liquid water in the anode compartment (pH ~ 7), or away from the ionomer, the concentration of HS^- would be close to the concentration of H_2S. Under all conditions, the concentration of S^{2-} would be vanishingly small. Calculation of the concentration of dissolved H_2S in the ionomer (assuming similar behavior to water) based on the free energy of hydration suggests that at the 100 ppm gaseous H_2S concentrations used in this study, an equilibrium H_2S concentration of 10.2×10^{-6} mol dm^{-3} will exist close to the catalyst. At such low concentrations of H_2S, it may be considered surprising that any S_{ads} would be deposited on the anode as the equilibrium potential for this reaction would be shifted to 0.289 V (RHE) [51]. Although the standard potential for decomposition of H_2S to S is well known [51], this potential is calculated assuming the product is elemental sulfur with the orthorhombic crystal structure and stoichiometry, S_8. However, the species adsorbed on platinum during the oxidation of H_2S is commonly considered to be adsorbed sulfur atoms, and as such the thermodynamics of that deposition may be somewhat different, eq (7) [52,53]. For instance, it is well known that thermodynamic underpotential deposition of adlayers of metals or other species may occur a few hundred millivolts away from the equilibrium potential due to the reduction in surface free energy [54–56]. It is also important to note that the effect of adsorbed sulfur at low coverages on the hydrogen adsorption features is striking – at low coverages of sulfur, each adsorbed sulfur atom blocks somewhere between 8 and 10 platinum atoms [52,53]. Hence, even low coverages of sulfur can significantly affect the hydrogen oxidation reaction. Furthermore, S_{ads} is not the only compound which can potentially be formed. During reaction of H_2S on platinum, it is possible to have oxidation of the platinum to form Pt^{II} and reaction with the sulfide to produce platinum (II) sulfide, and platinum (IV) sulfide, $Pt^{IV}S_2$. These reactions are analogous to the growth of platinum oxide at higher potentials (and in which the H_2S is replaced by H_2O). The standard electrochemical potentials for these processes, calculated from the free energies of formation of the platinum sulfides [57] and H_2S(aq) [51] are remarkably close to that of eq (5):

$$Pt^{II}S + 2H^+ + 2e^- \rightleftharpoons H_2S + Pt \quad E^o = 0.252\ V \quad (8)$$

$$Pt^{IV}S_2 + 4H^+ + 4e^- \rightleftharpoons 2H_2S + Pt \quad E^o = 0.116\ V \quad (9)$$

Evidence exists for the formation of $Pt^{II}S$ and $Pt^{IV}S_2$, although typically they seem to form at potentials greater than might be expected at a fuel cell anode [46,58]. Hence, in the following discussion we will refer to the species produced as S_{ads}.

Surprisingly, the 4th peak in the CV of the fresh electrode also disappears upon H_2S contamination. The suppression of the quinone/hydroquinone couple may be due to the reaction of the quinone group with the H_2S to form sulfur:

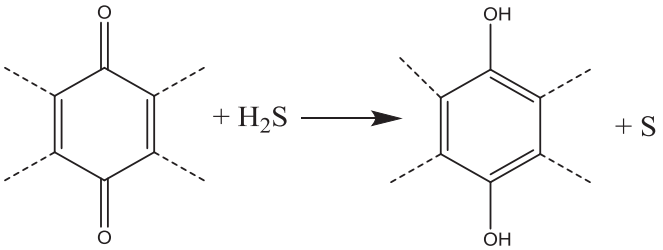

(10)

The sulfur produced would then prevent the reduction of the hydroquinone back to the quinone, so the electrochemical couple would disappear. The use of quinones or napthoquinones is well established as a method to remove H_2S from gas streams, as either the Stretford or Hyperion process, although in these cases the quinone/hydroquinone is dissolved in aqueous solution, and not attached to a carbon backbone. Hence there is no issue with the product sulfur blocking the active site [59].

Electrochemical cleaning of fuel cell electrode was accomplished by holding the potential of the electrode at a high potential at room temperature for various lengths of time. In order to assess what potential to use, we characterized the open circuit potential of a poisoned electrode during ozone exposure in the electrochemical cell at room temperature. Fig. 3(a) shows the shift in the OCP of the electrode during bubbling of ozone through the electrolyte. It is found that the presence of 2 vol% O_3 in the pure oxygen purging gas increased the OCP of the cell from 1.1 V under pure oxygen to 1.60 V after 900 s O_3 exposure. Experimentally, it is well known that elemental S can be oxidized electrochemically at potentials greater than 1.25 V vs RHE [28]. However, a complete recovery of the catalyst cannot be achieved by polarizing the cell electrochemically under fuel cell operating conditions [38]. For better understanding, we compare the cyclic voltammograms in aqueous sulfuric acid electrolyte of identical electrodes which have undergone H_2S contamination in the flowfield (Fig. 1(b)) and either ozone treatment in the flowfield or polarization at 1.60 V vs RHE in the sulfuric acid electrolyte for identical lengths of time, Fig. 3(b).

The CV of the electrochemically cleaned electrodes shows that the recovery of the sites responsible for the strongly adsorbed hydrogen peak is not as efficient as recovery of the sites associated with weakly bound hydrogen. It would appear that contamination of these former sites is more difficult to remove than contamination of the weakly adsorbed hydrogen sites. The shape of the CVs after 300 and 900 s polarization at 1.6 V are essentially the same. Only after 900 s polarization is there further growth of the strongly bound hydrogen peak. However, even at the longest polarization time, external polarization cannot recover all the hydrogen adsorption sites of the Pt catalysts. It has been known for some time that two forms of sulfur are adsorbed on platinum and that one form is more difficult to oxidize [42]. On the basis of XANES and

EXAFS analysis it is suggested that the easily oxidized sulfur is adsorbed on (111) facets of the platinum particles and the more difficult to remove sulfur is adsorbed on the (100) and edge sites [60], although experiments on (111) single crystal platinum also detect the presence of two types of sulfur [61].

Unlike external polarization, O_3 treatment at room temperature in the flowfield appears to affect the adsorbed sulfur differently. A 300 s treatment with O_3 in the flowfield (Fig. 1(b)) followed by returning the electrode to the electrochemical cell shows that both the weakly and strongly adsorbed hydrogen peaks are equally rejuvenated. Moreover, the efficiency of sulfur removal is much faster than the external polarization method. This suggests that O_3 not only affects oxidation of the sulfur adsorbate by increasing the electrochemical potential of the electrode but it also directly (or indirectly) reacts with the adsorbed sulfur. The ECSA of the fresh and cleaned electrodes are shown in Fig. 3(c). Unlike external polarization, O_3 rejuvenates the electrode completely within 900 s (each experiment performed on a fresh electrode with error bars in Fig. 3(c) corresponding to the standard deviation over 10 replicates of the experiment).

3.2. SO_2 evolution during O_3 cleaning

Fig. 4 shows the SO_2 and CO_2 evolution during O_3 cleaning of the H_2S contaminated electrodes at room temperature in the flowfield (Fig. 1(b)). O_3, SO_2 and CO_2 concentrations were measured simultaneously using the mass spectrometer. No CO_2 production is evident in the mass spectrum during O_3 exposure at room temperature.

Experiments were also performed at higher temperatures (70 and 80 °C), and the time-course for the SO_2 production trace was found to be similar (results not shown). It seems that increasing the temperature does not significantly improve the rate of S_{ads} oxidation, although it is known to significantly increase the rate of carbon corrosion. Hence, in all experiments performed, we have performed the O_3 treatments at room temperature to avoid excessive carbon corrosion.

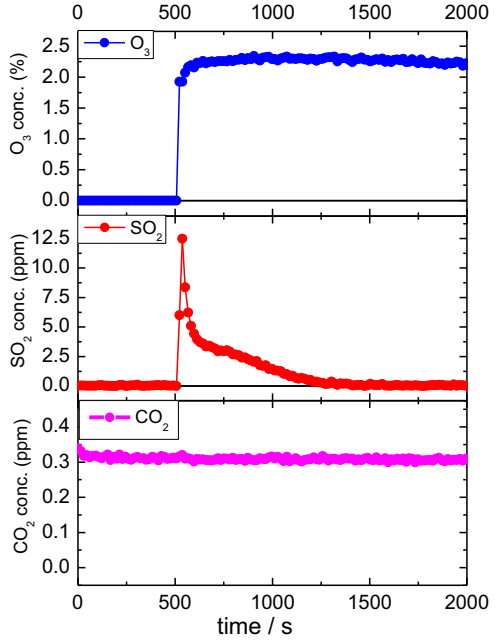

Fig. 4. SO_2 evolution during O_3 cleaning (O_3 in O_2) of H_2S contaminated (100 ppm H_2S, 900 s) fuel cell electrodes at room temperature. The CO_2 recorded in the gas analyzer during the O_3 cleaning process is shown in the bottom panel.

A transient signal for SO_2 is observed on switching the feed gas from O_2 to O_3/O_2. The SO_2 signal drops down to baseline levels after about 700 s of ozone exposure. Therefore, the SO_2 evolution profile replicates the effects seen for O_3 cleaned electrodes in that all sulfur appear to be effectively removed within 900 s of treatment. We cannot perform a quantitative mass balance analysis as we do not know the amount of H_2S adsorbed on the carbon of the electrodes, but we would expect a range of oxy-sulfur compounds produced during the ozone reaction, many of which would not be gaseous and would be eventually washed out in the fuel cell product water. Hence, SO_2 is a good proxy for the oxidation of adsorbed sulfur species, but in all likelihood SO_2 may not be the sole product. There is scant literature on the reaction mechanism of O_3 with elemental sulfur or metal sulfides on solid supports. As discussed in the previous section, it appears as if the O_3 cleaning mechanism can be broadly subdivided into electrochemical and chemical processes. The chemical process can be a combination of (a) direct reaction of ozone with the contaminant and (b) a series of complex indirect chemical reactions involving radical intermediates. The direct reaction does not require water and involves attack of the O_3 on Pt–S_{ads} to release SO_2 (eqs. (11) and (12)) or SO_3 (eq (13)).[1] We did not detect any gas phase SO_3, probably because sulfur trioxide is a liquid at the temperature of the experiment (melting point: 16.9 °C), and is much more acidic than sulfur dioxide and would thus undergo subsequent and rapid hydrolysis in the presence of any adventitious water to form sulfuric acid (eq. (14)).

$$Pt - S_{ads} + O_{3(g)} \rightarrow Pt - O + SO_{2(g)} \quad (11)$$

$$Pt - S_{ads} + O_{3(g)} \rightarrow Pt + SO_{2(g)} + O^{\cdot}_{(g)} \quad (12)$$

$$Pt - S_{ads} + O_{3(g)} \rightarrow Pt + SO_{3(l)} \quad (13)$$

$$SO_{3(l)} + H_2O_{(l)} \rightarrow H_2SO_{4(l)} \quad (14)$$

The indirect process, which occurs in the acidic aqueous environment of the ionomer, involves the formation of radical species and their subsequent attack on the adsorbed sulfur. Under acidic conditions, ozone reacts to produce an oxygen atom, followed by subsequent reaction with water to produce two hydroxyl radicals [62,63], (eqs (15) and (16)). The $O^{\bullet}$ and $OH^{\bullet}$ radicals may then react with Pt–S_{ads} to produce a range of sulfur containing species including the SO_2 which we detect using mass spectrometry. A possible first step is the production of the adsorbed intermediates, SO_{ads} or SOH_{ads}. This is then followed by subsequent oxidation by oxygen containing species represented as [O] (e.g. $O^{\bullet}$, $HO^{\bullet}$, O_2, H_2O etc) to sulfur oxides which desorb from the surface liberating the platinum surface, eq (17)–(19). The species $S_xO_y^{z-}$ is meant to represent the range of different species which can be produced (e.g. SO_2, SO_3, SO_3^{2-}, SO_4^{2-}, $S_2O_3^{2-}$ etc). As these are chemical reactions, for reasons of charge balance we must include the production of protons in equations (19) and (20) where the protons come from either $HO^{\bullet}$, or H_2O

$$O_{3(aq)} \rightarrow O_{2(aq)} + O^{\cdot}_{(aq)} \quad (15)$$

$$O^{\cdot}_{(aq)} + H_2O \rightarrow 2OH^{\cdot}_{(aq)} \quad (16)$$

$$Pt - S_{ads} + O^{\cdot}_{(aq)} \rightarrow Pt - SO_{ads} \quad (17)$$

[1] Although we list this as a gas phase reaction, it probably occurs via dissolution of ozone into the (aqueous) environment of the ionomer.

$$Pt - S_{ads} + OH^{\cdot}_{(aq)} \rightarrow Pt - SOH_{ads} \quad (18)$$

$$Pt - SO_{ads} + [O] \rightarrow Pt + S_xO_y^{z-} + zH^+ \quad (19)$$

$$Pt - SOH_{ads} + [O] \rightarrow Pt + S_xO_y^{z-} + zH^+ \quad (20)$$

The second way in which adsorbed sulfur containing intermediates can be oxidized is via an electrochemical mechanism which involves the simultaneous reduction of O_3. Ozone reduction may occur through either a 6, or 2- electron reduction producing either water, or oxygen as products [51]

$$O_3 + 6H^+ + 6e^- \rightleftharpoons 3H_2O \quad E^o = 1.511\ V \quad (21)$$

$$O_3 + 2H^+ + 2e^- \rightleftharpoons O_2 + H_2O \quad E^o = 2.076\ V \quad (22)$$

These reactions are then coupled to the simultaneous oxidation of the adsorbed sulfur with electron transfer occurring through the platinum/carbon of the catalyst layer, and proton transport through the ionomer:

$$SO_2 + 4H^+ + 4e^- \rightleftharpoons S + 2H_2O \quad E^o = 0.451\ V \quad (23)$$

$$SO_4^{2-} + 8H^+ + 8e^- \rightleftharpoons S + 4H_2O \quad E^o = 0.357\ V \quad (24)$$

where the standard potentials of the reactions are from Ref. [51]. In principle, there are a large number of possible oxidation products (as discussed above for the radical attack mechanism), and the process would occur in multiple steps, although we only list the overall stoichiometry for the processes which produces sulfur dioxide and sulphate, eqs (23) and (24). The driving force for this reaction is the difference in half-cell potentials between these two reactions ((21,22) and (23,24)) and is manifest as a difference in chemical potential of the protons in the ionomer at the two different reaction sites (as, to a first approximation, the potential drop seen by the electrons in the catalyst layer is negligible). Experimentally, it is found that potentials >1 V are required to oxidize sulfur from the platinum catalyst, implying that the kinetics of these reactions are quite slow and require a large overpotential to occur. During the O_3 treatment, the SO_2 produced does not redeposit on the platinum as the electrochemical potential is too high to allow reduction back to S.

3.3. *In-situ H_2S and O_3 cleaning*

Fig. 5(a) shows the polarization studies of the fuel cell operating on hydrogen/air at 70 °C under various conditions. It is observed that the performance of the fuel cell dropped drastically in the presence of 100 ppm H_2S as has been noted many times before. However, there is only a minor improvement in the performance of the cell after switching the anode fuel from H_2S/H_2 back to H_2. This appears to be due to blocking of hydrogen oxidation on the Pt catalyst due to S_{ads} adsorption. A comparison of the performance of the fuel cell after the various treatments described above compared to the fresh cell is shown in Fig. 5(b). Some scatter in these plots arise because we are taking the ratio of the cells performance however accuracy should be within ±2%. It is observed that the performance of the cell quickly drops to below 30% of that achievable in the fresh cell after a 900 s exposure to 100 ppm H_2S in H_2 (effective dose 23 μmol cm^{-2}). Treatment of the poisoned electrode rapidly restores performance. After only 300 s of O_3 treatment, at room temperature the performance of the fuel cell is 87–97% of the fresh cell across the entire current density range,

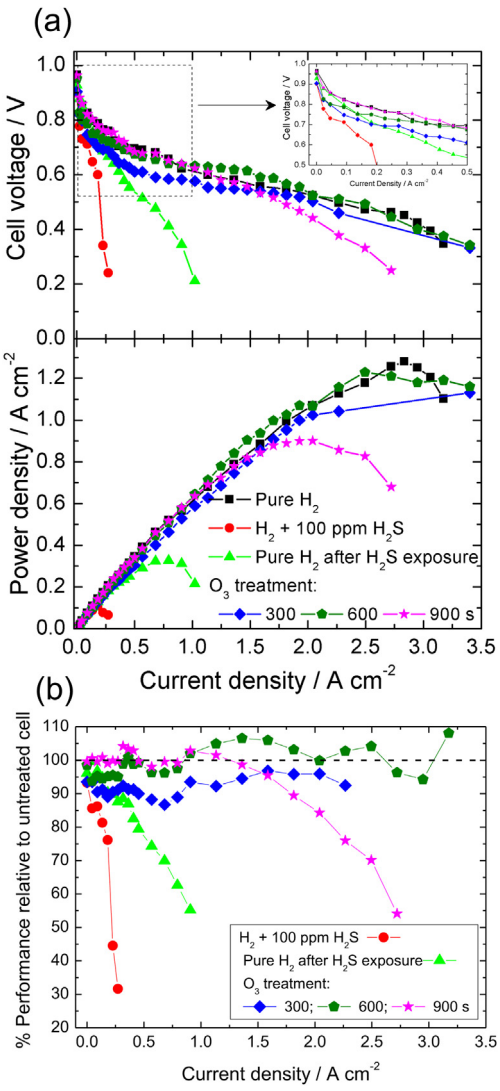

Fig. 5. (a) Polarization and power curves for a fuel cell operating on pure hydrogen (—■—), hydrogen + 100 ppm H_2S (—●—); pure hydrogen after exposure to 100 ppm H_2S (—▲—, effective dose 23 μmol cm^{-2}); pure hydrogen after 100 ppm H_2S poisoning and treatment with O_3 for 300 (—◆—), 600 (—⬟—) and 900 (—★—) seconds (b) Performance as a percentage of that achievable in the fresh cell (i.e. after break in and before H_2S exposure) derived from the results presented in (a). The. Fuel cell operated on H_2/air or H_2 + 100 ppm H_2S at 70 °C and 100%RH with no back-pressure with anode and cathode loadings of 0.4 mg cm^{-2}. Stoichiometries at 3.5 A cm^{-2} current density: anode:1.5; cathode: 2.5. Ozone treatment performed at room temperature.

with the lower values falling at the lower current densities. Extending the treatment to 600 s leads to fuel cell performance which is 97–108% of the fresh cell performance – evidently O_3 treatment may be beneficial in improving fuel cell performance to greater than initial values. The performance of the fuel cell is greater than the fresh cell for almost all current densities greater than 0.5 A cm^{-2}, although there are still some losses in the kinetic region, especially at current densities less than 0.25 A cm^{-2} (see inset graph expanding the low current density range in Fig. 5(a)). O_3 treatment for 900 s has both positive and negative effects. Within the kinetic region, and for current densities up to 1.4 A cm^{-2}, the performance is restored to that which the system had before exposure to hydrogen sulfide (i.e. 99–104% of initial performance) whereas at higher current densities there is a decrease in performance. This effect may be either due to the loss of Pt active sites

(although the similarity in kinetic region argues against this possibility) or due to increased mass transport losses due to a loss of hydrophobicity of the catalyst layer (see below). In Ref. [25], a 92% recovery of fuel cell performance at a cell potential of 0.6 V is achieved utilizing potential cycling. Utilizing a 600 s room temperature O_3 treatment, we find a significantly better recovery of performance – achieving a performance gain at 0.6 V cell potential (106%). Indeed, over the entire current density range studied – we see performance which is 97–108% of the fresh cell.

3.4. Durability studies of repeated H_2S contamination and O_3 cleaning

In order to assess the effect of repeated poisoning/cleaning cycles, we took a fresh MEA and established its performance to use as a baseline. We then went through a cycle of exposing the anode to 100 ppm H_2S/H_2 for 900 s at 0.5 A cm^{-2} current density, followed by purging the cell with N_2 and then measuring the fuel cell performance at a current density of 0.5 A cm^{-2} using hydrogen as a fuel. After purging the anode again with N_2, the anode was exposed to an "aggressive" strategy of 2% O_3 in O_2 for 900 s, after which the anode was again purged and tested on pure H_2. The durability studies of the fuel cell after successive H_2S contamination and O_3 treatment is shown in Fig. 6. The O_3 treatment can recover the performance of the PEMFC satisfactorily at a current density of 0.5 A cm^{-2} even after five poisoning/cleaning cycles. A marginal decrease in the performance of the cell was observed after each H_2S contamination and O_3 recovery cycle. This loss may be due to a loss of hydrophobicity. Franck-Lacaze et al. reported an increase in the diffusion resistance of the MEA after four doses of 1000 ppm O_3 for 720 s each [64]. They reported that the increase in diffusion resistance was attributed to the loss of ionomer around the catalyst clusters. However, O_3 exposure did not show significant effect on the bulk membrane. Such a possibility cannot be ruled out after repeated contamination and cleaning cycles.

3.5. Effect of O_3 cleaning on fuel cell performance

In order to better understand the mechanism behind the performance degradation at higher current densities, a fresh membrane electrode assembly was treated with O_3 for different lengths of time. Both current density-voltage and in-situ cyclic voltammetry

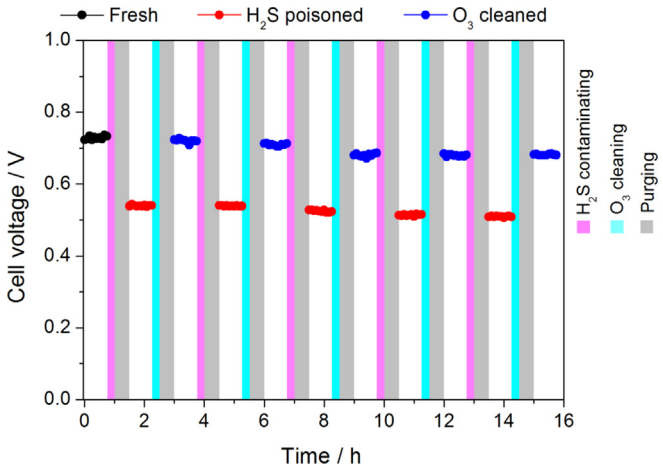

Fig. 6. Performance studies of PEMFC at 0.5 A cm^{-2} current density under successive 100 ppm H_2S poisoning (effective dose 23 μmol cm^{-2}) and 2% O_3 cleaning (900 s, room temperature). Fuel cell operated on H_2/air at 70 °C and 100%RH with no backpressure with anode and cathode loadings of 0.4 mg cm^{-2}. Stoichiometries at 3.5 A cm^{-2} current density: anode:1.5; cathode: 2.5.

experiments were performed as a function of successive 300 s O_3 treatments to assess the effect of the O_3 treatment on both the catalyst and fuel cell performance. These experiments were performed in the absence of any H_2S treatment in order to characterize the effect of O_3 alone on the performance of the fuel cell.

The polarization curves of the fresh PEMFC and for different O_3 treatment times is shown in Fig. 7(a), with the power versus current density in Fig. 7(b). There is a significant loss in performance at current densities greater than 1.0 A cm^{-2}, especially for longer ozone treatment times. There does not appear to be significant differences in the kinetic region of the IV curve as a function of ozone treatment (inset in Fig 7(a)). However, this is hardly surprising as the kinetic region is dominated by the cathode. Hence, in order to consider the anode in greater detail and look for some modification to the anode catalyst, we also performed in-situ cyclic voltammetry on the anode after each O_3 treatment time, Fig. 7(c). The specific catalyst area calculated from the hydrogen adsorption region corrected for double layer current before any O_3 exposure is around 20% less than that seen for the same electrode in sulfuric acid electrolyte (73 $m^2\ g^{-1}_{Pt}$ compared to 89 $m^2\ g^{-1}_{Pt}$ in Fig. 3) probably due to the decreased utilization of platinum in solid state systems. Furthermore, after 1200 s of O_3 treatment, there is a reduction of electrochemical surface area of about 10%. It would appear that although the O_3 degrades the Pt–catalyst or carbon support, this effect is relatively slow, and would not be expected to significantly affect the electrokinetics of the hydrogen oxidation reaction. This surface area reduction is almost certainly due to carbon corrosion and platinum dissolution and redeposition.

Comparing the results shown in Fig. 7(a) with those in Fig. 5(a) shows that within the limits of our experimental measurements, there is no difference in the performance at high current density between electrodes that have been O_3-treated and those that have been exposed to H_2S and O_3 treated. Hence, it would appear that the degradation of performance at high current density is predominantly due to the O_3 exposure and probably associated with degradation of the water handling properties or collapse of the porous structure of the electrodes. We have already shown in Fig. 4 that we do not detect significant amounts of carbon dioxide during the ozone treatment as we intentionally perform the cleaning process at room temperature. In order to test the first of these two hypotheses, we examined the time-varying static water contact angle on the catalyst sides of electrodes before H_2S treatment, after H_2S treatment, and as a function of the ozone treatment time, Fig. 8. Measurement of contact angles on rough surfaces is fraught with difficulties due to issues associated with significant variation in advancing and receding contact angles, and the formation of Cassie–Baxter or Wenzel states [65]. Nonetheless, we consider that such measurements are useful in providing some insight into the wetting behavior of the electrodes. Placing water on a porous substrate will produce an apparent contact angle (θ_D) related to the solid-water interfacial area (f_1), the water–air interfacial area (f_2) and the advancing contact angle of the water on the solid (θ_A) such that [65]

$$\cos\theta_D = f_1 \cos\theta_A - f_2 \tag{25}$$

Hence large perceived contact angles are favored by large water-solid contact angles (especially greater than 90°), and large water–air interfacial areas. The former is affected by the chemical structure of the catalyst layer whereas the latter is mostly influenced by the porosity of the catalyst layer. An untreated fuel cell electrode shows a time independent super-hydrophobic contact angle of 138°, Fig. 8. This is hardly surprising as some hydrophobic materials are introduced into catalyst layers to control their water handling properties (e.g. the advancing contact angle of water on ptfe is

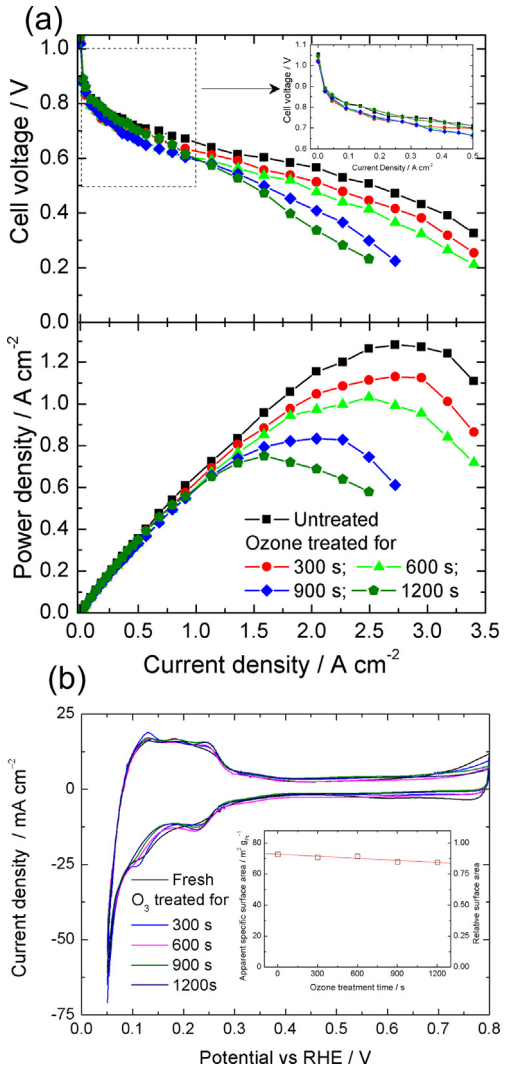

Fig. 7. (a) Fuel cell IV-curves for different 2% O_3 in O_2 treatment times; and corresponding power density curves. (—■—), untreated; Ozone treated for 300 s, (—●—); 600 s, (—▲—v); 900 s, (—◆—); 1200 s, (—⬟—). Fuel cell operated on H_2/air at 70 °C and 100%RH with no backpressure with anode and cathode loadings of 0.4 mg cm^{-2}. Stoichiometries of anode:1.5; cathode: 2.5. Ozone treatment performed at room temperature. (b) In-situ IV curves of the anode catalyst in the fuel cell under a nitrogen atmosphere showing the hydrogen adsorption region. Inset: variation of the specific catalyst surface area with O_3 treatment time. Operating conditions are temperature: 35 °C, H_2 and N_2 flow rate 50 sccm, no backpressure, and scan rate: 40 mV s^{-1}.

110°). Treating that surface with 100 ppm H_2S for 900 s leads to a surface which is less hydrophobic (124°) and which shows a decrease in hydrophobicity with time (reaching 120° after 300 s). The slow decrease of contact angle over time is probably indicative of slow ingress of water into the catalyst layer. Water has an advancing contact angle on Sulfur of 89.7° [66], and so it might be expected that on deposition of sulfur in the catalyst layer, a decrease of θ_D occurs in line with equation (25). Treatment of this contaminated catalyst layer with O_3 for 900 s restores much of the hydrophobicity, and leads to a time invariant contact angle of 132°. Taking a fresh electrode and treating with O_3 for 1200 s also leads to a significant decrease in hydrophobicity and a decay in the contact angle with time. Hence long term ozone treatment clearly shows some deleterious effect on the water handling capability of the catalyst layer. Hence O_3 treatment is a double-edged sword — although it effectively remediates electrodes from H_2S poisoning, it

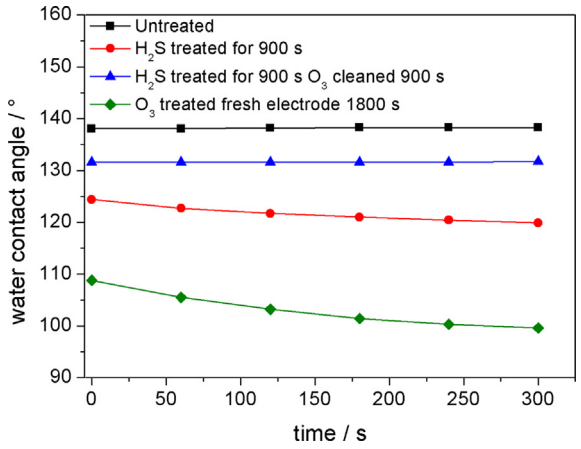

Fig. 8. Contact angle measurement on fuel cell electrodes after exposure to 100 ppm H_2S in H_2 and 2% O_3 in O_2 for different treatment times. All chemical treatments performed at 25 °C.

also leads to a reduction in water handling properties. Ultimately, there is greater benefit in being able to operate a fuel cell after H_2S exposure but with a slight loss of performance at high current density due to the reduced water handling properties, than not being able to operate the fuel cell at all.

In passing, we note that the reduction in water handling properties and decay in catalyst surface area may indicate that exposure to O_3 is a good proxy for what happens to fuel cells after long times. Hence, O_3 exposure may be used to rapidly assess the long term degradation of electrodes and how their properties change with time.

4. Conclusions

In this paper we have shown that room-temperature ozone treatment is an effective method for removing H_2S contamination of fuel cell anodes in both ex-situ and in-situ experiments. This process is interesting as it could be simply and directly applied to fuel cell stacks with a minimum of extra equipment and provide a simple method for remediating systems exposed to H_2S. As SO_2 poisoning of fuel cells produces the same contaminant species, this approach would also be useful to remediate fuel cells exposed to SO_2. It is found that during O_3 exposure, the open-circuit potential of a fuel cell electrode rises to about 1.6 V vs RHE. During ozone exposure, a characteristic spike in SO_2 production is observed, and this SO_2 production is correlated with the loss of contaminant from the fuel cell electrode surface. It is found that the mechanism of O_3 reaction with chemisorbed contaminants (S_{ads}) is somewhat different to that of electrochemical polarization and leads to more complete cleaning of the electrode for equivalent treatment times. Hence it appears as if there is a chemical process occurring as well as an electrochemical process. Electrochemical oxidation appears to preferentially remove S_{ads} blocking the platinum sites associated with weakly-bound hydrogen whereas those sites associated with strongly-bound hydrogen are more slowly cleaned. The chemical process may either be due to direct reaction of ozone with S_{ads}, or due to the intermediate formation of radical species ($O^{\bullet}$, $HO^{\bullet}$ etc) which then undergo reaction with S_{ads}. The chemical process appears to be more indiscriminate and leads to removal of S_{ads} from all sites at a uniform rate. It appears as if it is possible to completely recover an electrode using O_3, whereas the electrochemical polarization process always leaves a small amount of S_{ads} on the electrode. We also note that there is some effect of H_2S on the hydroquinone/quinone electrochemical couple on the carbon

supports. Complete S_{ads} removal is confirmed after about 900–1200 s 2% O_3 treatment by both cessation of SO_2 production, total recovery of the platinum electrochemical surface area and recovery of the fuel cell IV curve and performance. The recovery process can be utilized multiple times, although there is slight loss in performance after each successive poisoning/remediation cycle. This performance loss is not due to the H_2S treatment but rather to cumulative exposure to O_3 as confirmed by independent exposure of electrodes to O_3 for different lengths of times. The loss in performance appears to be probably due to a decrease in hydrophobicity of the catalyst layer as determined from static contact angle measurements. It is interesting to note that the O_3 treatment process may represent a useful approach for accelerated durability testing of fuel cell catalyst layers.

Acknowledgments

The authors would like to acknowledge the Engineering and Physical Sciences Research Council for funding under project EP/I037024/1.

Appendix A. Supplementary data

Supplementary data related to this article can be found at http://dx.doi.org/10.1016/j.jpowsour.2013.11.077.

References

[1] S.G. Chalk, J.F. Miller, F.W. Wagner, J. Power Sources 86 (2000) 40–51.
[2] P. Costamagna, S. Srinivasan, J. Power Sources 102 (2001) 242–252.
[3] J. Larminie, A. Dicks, M.S. McDonald, Fuel Cell Systems Explained, Wiley Chichester, 2003.
[4] J.M. Ogden, Annu. Rev. Energy Env. 24 (1999) 227–279.
[5] D. Yang, J. Ma, J. Qiao, CRC Press, 2010, pp. 115–150.
[6] J.C. Amphlett, R.M. Baumert, R.F. Mann, B.A. Peppley, P.R. Roberge, A. Rodrigues, Prepr. Pap. Am. Chem. Soc. Div. Fuel Chem. 38 (1993) 1477–1481.
[7] A. Rodrigues, J.C. Amphlett, R.F. Mann, B.A. Peppley, P.R. Roberge, Proc. Intersoc. Energy Convers. Eng. Conf. 32nd (1997) 768–773.
[8] R.J. Bellows, E. Marucchi-Soos, R.P. Reynolds, Electrochem. Solid-State Lett. 1 (1998) 69–70.
[9] J.J. Baschuk, X. Li, Int. J. Energy Res. 25 (2001) 695–713.
[10] G.A. Camara, E.A. Ticianelli, S. Mukerjee, S.J. Lee, J. McBreen, J. Electrochem. Soc. 149 (2002) A748–A753.
[11] A. Manasilp, E. Gulari, Appl. Catal. B 37 (2002) 17–25.
[12] K. Narusawa, M. Hayashida, D. Kurashima, K. Wakabayashi, Y. Kamiya, JSME Int. J. Ser. B 46 (2003) 643–649.
[13] E.I. Santiago, M.S. Batista, E.M. Assaf, E.A. Ticianelli, J. Electrochem. Soc. 151 (2004) A944–A949.
[14] L.Y. Sung, Y.Y. Yan, H.S. Chu, R.J. Shyu, F. Chen, in: R.K. Shah, S.G. Kandlikar (Eds.), Second International Conference on Fuel Cell Science, Engineering and Technology American Society of Mechanical Engineers, Rochester, New York, 2004, pp. 621–624.
[15] W.A. Adams, J. Blair, K.R. Bullock, C.L. Gardner, J. Power Sources 145 (2005) 55–61.
[16] I. Rosso, C. Galletti, S. Fiorot, G. Saracco, E. Garrone, V. Specchia, J. Porous Mater. 14 (2007) 245–250.
[17] W. Wang, J. Power Sources 191 (2009) 400–406.
[18] L.-Y. Sung, B.-J. Hwang, K.-L. Hsueh, F.-H. Tsau, J. Power Sources 195 (2010) 1630–1639.
[19] S.-i. Yamazaki, M. Yao, Z. Siroma, T. Ioroi, K. Yasuda, J. Phys. Chem. C 114 (2010) 21856–21860.
[20] A. Pitois, J.C. Davies, A. Pilenga, A. Pfrang, G. Tsotridis, J. Catal. 265 (2009) 199–208.
[21] R. Mohtadi, W.K. Lee, S. Cowan, Z.J.W. Van, M. Murthy, Electrochem. Solid-State Lett. 6 (2003) A272–A274.
[22] Y. Takagi, F. Nakatani, M. Okamoto, T. Shimizu, S. Hikita, Soc. Automot. Eng. (2004) 173–179 [Spec. Publ.] SP, SP-1827.
[23] I.G. Urdampilleta, F.A. Uribe, T. Rockward, E.L. Brosha, B.S. Pivovar, F.H. Garzon, ECS Trans. 11 (2007) 831–842.
[24] M. Shen, D. Yang, J. Wang, Z. Gong, W. Zhou, J. Ma, J. Xi'an Jiaotong Univ. 42 (2008) 1054–1058.
[25] B.D. Gould, O.A. Baturina, K.E. Swider-Lyons, J. Power Sources 188 (2009) 89–95.
[26] S. Mu, F. Xu, Wuhan University of Technology, Peop. Rep. China, 2010, p. 13.
[27] F.A. Uribe, T.A. Zawodzinski, Jr., 2001, Medium: ED, Size: 2 p.
[28] T. Loucka, J. Electroanal. Chem. 31 (1971) 319–332.
[29] T. Loucka, J. Electroanal. Chem. 36 (1972) 369–381.
[30] A. Heinzel, W. Benz, F. Mahlendorf, O. Niemzig, J. Roes, in: Proceedings of the 2002 Fuel Cell Seminar, Palm Springs, California, USA, 2002, pp. 149–152.
[31] F.H. Garzon, T. Lopes, T. Rockward, J.-M. Sansinena, B. Kienitz, R. Mukundan, T. Springer, ECS Trans. 25 (2009) 1575–1583.
[32] B.D. Gould, G. Bender, K. Bethune, S. Dorn, O.A. Baturina, R. Rocheleau, K.E. Swider-Lyons, J. Electrochem. Soc. 157 (2010) B1569–B1577.
[33] R. Mohtadi, W.K. Lee, Z.J.W. Van, J. Power Sources 138 (2004) 216–225.
[34] K. Narusawa, K. Myong, K. Murooka, Y. Kamiya, SAE Int. (2007) 73–82 [Spec. Publ.] SP, SP-2098.
[35] W. Shi, B. Yi, M. Hou, P. Ming, F. Jing, Sunrise Power Co., Ltd., Peop. Rep. China, 2008, p. 8.
[36] W. Shi, B. Yi, M. Hou, Z. Shao, Int. J. Hydrogen Energy 32 (2007) 4412–4417.
[37] Z. Shi, D. Song, J. Zhang, Z.-S. Liu, S. Knights, R. Vohra, N. Jia, D. Harvey, J. Electrochem. Soc. 154 (2007) B609–B615.
[38] V.A. Sethuraman, J.W. Weidner, Electrochim. Acta 55 (2010) 5683–5694.
[39] W. Shi, B. Yi, M. Hou, F. Jing, P. Ming, J. Power Sources 165 (2007) 814–818.
[40] W. Shi, B. Yi, M. Hou, F. Jing, H. Yu, P. Ming, J. Power Sources 164 (2007) 272–277.
[41] R. Mohtadi, W.K. Lee, J.W. Van Zee, Appl. Catal. B 56 (2005) 37–42.
[42] A. Contractor, H. Lal, J. Electroanal. Chem. 96 (1979) 175–181.
[43] T.R. Ralph, G.A. Hards, J.E. Keating, S.A. Campbell, D.P. Wilkinson, M. Davis, J. StPierre, M.C. Johnson, J. Electrochem. Soc. 144 (1997) 3845–3857.
[44] K. Rakness, G. Gordon, B. Langlais, W. Masschelein, N. Matsumoto, Y. Richard, C.M. Robson, I. Somiya, Ozone-Sci. Eng. 18 (1996) 209–229.
[45] A. Parthasarathy, S. Srinivasan, A.J. Appleby, C.R. Martin, J. Electroanal. Chem. 339 (1992) 101–121.
[46] E. Najdeker, E. Bishop, J. Electroanal. Chem. 41 (1973) 79–87.
[47] F.G. Will, J. Electrochem. Soc. 112 (1965) 451–455.
[48] T. Frelink, W. Visscher, J. Van Veen, Electrochim. Acta 40 (1995) 545–549.
[49] B. Avasarala, R. Moore, P. Haldar, Electrochim. Acta 55 (2010) 4765–4771.
[50] M.-V. Mathieu, M. Primet, Appl. Catal. A 9 (1984) 361–370.
[51] M.J.N. Pourbaix, Atlas of Electrochemical Equilibriums in Aqueous Solutions, second ed., Natl. Assoc. Corrosion Engs, 1974.
[52] E. Protopopoff, P. Marcus, J. Chim, Phys. Phys.-Chim. Biol. 88 (1991) 1423–1452.
[53] Y.-E. Sung, W. Chrzanowski, A. Zolfaghari, G. Jerkiewicz, A. Wieckowski, J. Am. Chem. Soc. 119 (1997) 194–200.
[54] L.P. Colletti, D. Teklay, J.L. Stickney, J. Electroanal. Chem. 369 (1994) 145–152.
[55] E. Lamy-Pitara, J. Barbier, Appl. Catal. A 149 (1997) 49–87.
[56] E. Lamy-Pitara, L. Bencharif, J. Barbier, Appl. Catal. A 18 (1985) 117–131.
[57] D. Lide, CRC Handbook of Chemistry and Physics, 87 ed., CRC Press, Boca Raton, FL, 2007.
[58] N. Ramasubramanian, J. Electroanal. Chem. 64 (1975) 21–37.
[59] R.A. Douglas, Am. Chem. Soc. Div. Fuel Chem. 35 (1990) 136–149.
[60] D.E. Ramaker, D. Gatewood, A. Korovina, Y. Garsany, K.E. Swider-Lyons, J. Phys. Chem. C 114 (2010) 11886–11897.
[61] J.A. Rodriguez, M. Kuhn, J. Hrbek, Chem. Phys. Lett. 251 (1996) 13–19.
[62] K. Sehested, H. Corfitzen, J. Holcman, C.H. Fischer, E.J. Hart, Environ. Sci. Technol. 25 (1991) 1589–1596.
[63] K. Sehested, H. Corfitzen, J. Holcman, E.J. Hart, J. Phys. Chem. 96 (1992) 1005–1009.
[64] L. Franck-Lacaze, C. Bonnet, S. Besse, F. Lapicque, Fuel Cells 9 (2009) 562–569.
[65] A.B.D. Cassie, S. Baxter, Trans. Faraday Soc. 40 (1944) 546–551.
[66] E. Chibowski, K. Terpilowski, J. Colloid Interface Sci. 319 (2008) 505–513.